Int. J. Pharm. Investigation, 2026; 16(3):1005-1017.
https://www.jpionline.org

Original Article

Fabrication and *in vitro-ex vivo* Evaluation of Diclofenac Sodium Transdermal Patches for Enhanced Skin Compatibility

Muhammad Abid Mustafa[1,*], Asad Majeed Khan[1], Ayesha Atif[1], Fatima Wajid[1], Nasir Ali[2], Khuram Ashfaq[3], Muhammad Abuzar Ghaffari[3], Nabeela Jabeen[4], Rabbia Nasir[1], Faiza Arshad[1], Laiba Kaleem[1]

[1]Department of Pharmaceutics, Faculty of Pharmaceutical Sciences, Lahore University of Biological and Applied Sciences, Lahore, PAKISTAN.
[2]Department of Pharmacy, Forman Christian College, University, Lahore, PAKISTAN.
[3]Department of Pharmaceutical Chemistry, Faculty of Pharmaceutical Sciences, Lahore University of Biological and Applied Sciences, Lahore, PAKISTAN.
[4]Department of Pharmacognosy, Faculty of Pharmaceutical Sciences, Lahore University of Biological and Applied Sciences, Lahore, PAKISTAN.

ABSTRACT

Background: Transdermal drug delivery systems provide a sophisticated and patient-compliant strategy for arthritis management by maintaining consistent plasma concentrations, reducing dosing frequency, and minimizing gastrointestinal adverse effects commonly associated with oral nonsteroidal anti-inflammatory drugs. **Aim and Objectives:** This study aimed to develop and optimize a controlled-release transdermal system of diclofenac sodium capable of sustaining therapeutic plasma levels, enhancing patient adherence, and improving treatment efficacy compared with conventional oral dosage forms. **Materials and Methods:** Diclofenac sodium patches were fabricated using the solvent-casting technique with Hydroxypropyl Methylcellulose (HPMC) and polyvinylpyrrolidone K-30 (PVP K-30) as film-forming polymers, polyethylene glycol 6000 (PEG-6000) as a plasticizer, and Sodium Lauryl Sulfate (SLS) as a permeation enhancer. Nine Formulations (F1-F9) were evaluated for physicochemical parameters including thickness, weight uniformity, folding endurance, drug content, and moisture content. Drug–polymer compatibility and structural integrity were assessed using FTIR, DSC, TGA, and SEM. *In vitro* release studies were performed in Phosphate buffer (pH 7.4), and kinetic modeling was conducted using zero-order, first-order, and Higuchi equations to elucidate the release mechanism. **Results and Discussion:** All formulations displayed satisfactory physicochemical properties with uniform drug distribution and matrix stability. FTIR, DSC, and TGA confirmed the absence of drug–polymer interactions, while SEM micrographs revealed smooth and homogeneous surface morphology. *In vitro* studies demonstrated sustained release up to 9 hr, with F4, F5, and F6 showing the highest cumulative release (89.54%, 94.14%, and 94.57%, respectively). Drug release followed zero-order kinetics (R^2=0.9313–0.989), indicating a concentration-independent, non-Fickian mechanism involving both diffusion and polymer relaxation. Skin irritation testing demonstrated excellent dermal compatibility, with a Primary Irritation Index (PII) < 0.4. According to Draize classification, the patches were non-irritant and safe for dermal application. **Conclusion:** Diclofenac sodium transdermal patches formulated with HPMC and PVP K-30 exhibited desirable physicochemical and kinetic properties, with F5 and F6 showing superior sustained-release performance. The non-irritant profile and stable matrix characteristics underscore their potential as effective and safe candidates for transdermal therapy in arthritis management.

Keywords: Diclofenac sodium, Transdermal patches, Controlled Release, HPMC, Zero-order kinetics, Arthritis management, Dermal Compatibility.

Correspondence:
Dr. Muhammad Abid Mustafa
Department of Pharmaceutics, Faculty of Pharmaceutical Sciences, Lahore University of Biological and Applied Sciences, Lahore, PAKISTAN.
Email: abidbhatti222@gmail.com
ORCID: 0009-0009-2851-3047

Received: 03-12-2025;
Revised: 16-01-2026;
Accepted: 27-03-2026.

INTRODUCTION

The Transdermal Drug Delivery System (TDDS) has gained interest for administering drugs through the skin, targeting localized skin conditions and delivering drugs into systemic circulation (Prajapati *et al.*, 2011). Transdermal delivery is an easy-to-use option suitable for all ages. This method improves drug bioavailability in the bloodstream, outperforming traditional drug delivery methods (Alkilani *et al.*, 2022). Transdermal patches effectively bypass hepatic first-pass metabolism, allowing

OPEN ACCESS

Manuscript TECHNOMEDIA

DOI: 10.5530/ijpi.20260145

the drug to enter systemic circulation through the skin directly (Ramadon *et al.*, 2022).

The transdermal drug delivery system delivers lipophilic, hydrophilic, and amphiphilic drugs to targeted sites for therapeutic action (Akhtar *et al.*, 2020). TDDS minimizes the risk of side effects, including nausea, emesis, and gastrointestinal irritation (Fong Yen *et al.*, 2015).

Osteoarthritis is the most common form of chronic degenerative disease, characterized by pain, inflammation, and reduced joint function. It negatively impacts the patient's quality of life (Singh *et al.*, 2024). It primarily affects the knee joints, leading to significant disability and morbidity that diminishes the quality of life for individuals suffering from a condition known as knee osteoarthritis (Sin *et al.*, 2025). This pain is accompanied by fatigue, restlessness, sensations with a needle-like quality, and dull pain (Törnblom *et al.*, 2024). According to a comprehensive Global Burden of Disease (GBD) assessment conducted in 2021, approximately 607 million individuals worldwide were estimated to be affected by Osteoarthritis (OA) across all joint sites. Furthermore, evidence from an extensive meta-analysis indicates that the global prevalence of knee osteoarthritis is roughly 16% among individuals aged 15 years and older, with the rate increasing to nearly 23% in populations aged 40 years and above. The burden of knee osteoarthritis is growing each day, projected to increase by 74.9% by 2050 due to various factors, including obesity, inactivity, a sedentary lifestyle, and poor diet habits (Cui *et al.*, 2020; Zhu *et al.*, 2024).

Diclofenac sodium is classified as a Non-Steroidal Anti-Inflammatory Drug (NSAID) within the phenylacetic acid derivative class. It is commonly prescribed for treating pain and inflammation related to conditions such as osteoarthritis, rheumatoid arthritis, and ankylosing spondylitis (Brogden *et al.*, 1980). Diclofenac inhibits COX-1 and COX-2 enzymes, which produce prostaglandins involved in inflammation and fever. Diclofenac sodium is the first-line therapy for knee osteoarthritis. While topical forms of diclofenac sodium and ketoprofen are common, diclofenac sodium is the main treatment choice (Wolff *et al.*, 2021). Diclofenac sodium possesses suitable physicochemical attributes for transdermal delivery, including a molecular weight of 318.13 g/mol, log P ≈ 4.0, and pKa ≈ 4.0, ensuring balanced solubility and permeability. Its high melting point (≈283°C) provides thermal stability for patch fabrication. These properties support its use in controlled-release transdermal systems that sustain plasma levels and provide localized anti-inflammatory action. Transdermal delivery also avoids first-pass metabolism, minimizes gastrointestinal effects, and, owing to the drug's short half-life (1-2 hr), enables prolonged therapeutic action and improved patient adherence in chronic arthritis management (Adamiak-Giera *et al.*, 2025).

The present study aims to design and optimize controlled-release transdermal patches of diclofenac sodium using a synergistic blend of semisynthetic and synthetic polymers to achieve sustained drug delivery for long-term pain management in osteoarthritis. The formulation is engineered to provide extended drug release through a diffusion-controlled mechanism, facilitating efficient percutaneous absorption while minimizing dosing frequency. Incorporation of permeation enhancers is intended to further augment transdermal flux and bioavailability. Comprehensive *in vitro* physicochemical and performance evaluations will be conducted to assess patch uniformity, mechanical integrity, drug content, release kinetics, and skin compatibility. The proposed transdermal system is expected to deliver prolonged analgesic and anti-inflammatory effects, reducing systemic adverse reactions and overcoming the limitations of conventional oral NSAID therapy, thereby improving therapeutic efficacy and patient adherence in osteoarthritis management.

MATERIALS AND METHODS

Materials

Diclofenac sodium ($C_{14}H_{10}Cl_2NNaO_2$; CAS No. 15307-79-6) was used as the model drug. The polymeric matrix was formulated using Hydroxypropyl Methylcellulose (HPMC; CAS No. 9004-65-3) and Polyvinylpyrrolidone K-30 (PVP K-30; CAS No. 9003-39-8) as film-forming polymers. Polyethylene Glycol 6000 (PEG 6000; CAS No. 25322-68-3) was incorporated as a plasticizer to enhance elasticity and homogeneity of the films. Sodium Lauryl Sulfate (SLS; CAS No. 151-21-3) acted as a permeation enhancer and surfactant, facilitating diffusion of the drug through the stratum corneum by modifying lipid bilayer permeability. Distilled water served as the solvent for uniform dissolution of the active and excipient components. All materials were of analytical and pharmaceutical grade (≥ 99% purity), procured from Sigma-Aldrich (Germany), and used without further modification.

Methods

Transdermal patches of diclofenac sodium were prepared following the method reported by Singh *et al.*, with minor modifications to optimize polymer compatibility and film uniformity. Accurately weighed quantities of Diclofenac Sodium (DS), PVP K-30, PEG-6000, HPMC, and Sodium Lauryl Sulfate (SLS) were obtained using a calibrated analytical balance, and each material was handled under controlled storage conditions to maintain integrity. The polymers were individually dissolved in 10 mL of distilled water to form uniform solutions. Because PVP K-30 and PEG-6000 exhibit limited solubility in cold water, while HPMC tends to form gels in hot water, the dissolution process was conducted at a carefully optimized temperature range to ensure complete polymer solubilization and to prevent premature gelation. Separately, diclofenac sodium (130 mg) and sodium lauryl sulfate (100 mg) were dissolved in 10 mL

of distilled water each. PEG-6000 was then incorporated into the PVP K-30 solution, followed by the gradual addition of HPMC with continuous mild stirring to avoid clump formation. The drug and SLS solutions were subsequently added to the polymer blend and stirred gently to achieve homogeneity while minimizing air entrapment. The resulting degassed polymeric dispersion was poured into pre-prepared aluminum-lined Petri dishes and tapped gently to ensure uniform layer distribution. The films were dried in a hot-air oven at 45°C until complete solvent evaporation. Dried patches were carefully peeled from the aluminum backing and cut into uniform squares (4.5 × 4.5 cm). A total of nine formulations were developed in accordance with the established Standard Operating Procedures (SOPs). The composition of each formulation is presented in Table 1 (Singh & Bali, 2016).

CHARACTERIZATION

Physical Appearance of the Patch

The patches were evaluated for organoleptic properties, including colour, surface texture and smoothness and clarity (Abdullah *et al.*, 2023).

Patch Thickness

A screw gauge was employed to measure the thickness accurately, and multiple measurements were made along the length of the patch (Alkilani *et al.*, 2015).

Percentage Elongation Break Test

The initial length of the patch was measured using a calibrated scale. A gradually increasing force was applied until rupture, and the final length was recorded. The percentage elongation at break was calculated using the standard formula (Shailesh T *et al.*, 2011).

$$Percentage\ elongation = \frac{Length\ increased}{Initial\ length} \times 100$$

Weight Variation

Weight uniformity was determined by cutting each patch into three equal segments (2 × 2 cm), weighing them individually, and expressing the results as the mean ± standard deviation (Mamatha *et al.*, 2020).

Flatness Study

Flatness was evaluated by cutting three longitudinal strips from each patch (one central and two peripheral). The length of each strip was measured, and any deviation in flatness was quantified as percentage constriction using the established formula (Kumar *et al.*, 2013).

$$Percentage\ constriction = \frac{\text{Final length of strip} - \text{Initial length of strip}}{\text{Final length of strip}} \times 100$$

Folding Endurance

Each patch was folded repeatedly at the same spot until it tore, and the number of folds before breaking was measured as folding endurance (Singh & Bali, 2016).

Swelling Index

Swelling Index (SI) was evaluated by immersing pre-weighed patches in phosphate buffer (pH 5.8) for 24 hr, followed by reweighing after excess surface fluid was removed (Subedi & MeenakshiKandwal). The swelling index was calculated using this formula.

$$SI = \frac{\{Wt.of\ swelling\ patch\ after\ 24\ hours\ (W2) - Initial\ wt.\ of\ patch\ before\ swelling\ (W1)}{Initial\ weight\ of\ patch\ before\ swelling\ (W1)} \times 100$$

Percentage Moisture Content

Each patch was accurately weighed, stored in a $CaCl_2$ desiccator at room temperature for 24 hr, and reweighed until a constant weight was achieved. The percentage of moisture content was calculated using the following formula (Zhang *et al.*, 2014).

$$Percentage\ of\ moisture\ Content = \frac{\text{Initial weight (Wi)} - \text{Final weight (Wf)}}{\text{Initial weight (Wi)}} \times 100$$

Surface pH

Patches were equilibrated in 0.5 mL of distilled water for 1 hr, and the surface pH was measured by gently placing a glass electrode on the swollen surface after 1 min of stabilization (Singh & Bali, 2016).

Standard Calibration Curve

A stock solution of diclofenac sodium (1 mg/mL) was prepared by dissolving 100 mg in 100 mL of distilled water. Serial dilutions were analyzed using UV spectrophotometry at 276 nm to construct the calibration curve (Abdul, 2025).

Drug Content Analysis

Each patch was cut into 1 × 1 cm sections and immersed in 100 mL of phosphate buffer (pH 7.4) with continuous stirring for 12 hr to extract the drug. The solution was sonicated for 20 min, filtered through Whatman filter paper, and an aliquot of 3 mL was suitably diluted. The drug content was determined spectrophotometrically at 276 nm, using a placebo patch extract as the blank. Quantification was performed using the standard calibration curve equation of diclofenac sodium. The equation used is as follows (Subedi & MeenakshiKandwal).

$$\%\ \text{Drug Content} = \frac{Drug\ Content\ in\ Patch\ (mg)}{Total\ Drug\ Loaded\ into\ Patch\ (mg)}\ x\ 100$$

Fourier Transform Infrared Spectroscopy (FTIR) Analysis

FTIR spectroscopy was performed for pure diclofenac sodium, drug-loaded, and placebo patches using a standard FTIR spectrophotometer (Cary-630, Agilent Technologies). Samples

of appropriate particle size were prepared and analyzed over a wavelength range of 4000–500 cm^{-1} with a transmittance range of 30–100% to identify possible drug–polymer interactions and confirm chemical compatibility within the formulation (Shafique *et al.*, 2021).

Scanning Electron Microscopy (SEM)

The surface morphology and structural features of the patches were examined using a Scanning Electron Microscope (EVO LS 10, Zeiss, Germany). Prior to imaging, samples were mounted on aluminum stubs using double-sided conductive adhesive tape and sputter-coated with a thin layer of gold under vacuum to enhance surface conductivity and image resolution (Nayak *et al.*, 2011).

Thermal Analysis

Thermal characterization was performed using a Q600 TA Instruments (USA) system. For DSC, approximately 2.5–5 mg of each sample was sealed in an aluminum crucible and heated from room temperature to 500°C at 10°C/min under nitrogen. For TGA, about 3 mg of sample was heated over the same temperature range at 5°C/min. Thermal transitions and weight-loss profiles were recorded to assess thermal stability and drug–excipient compatibility within the formulations (Tudja *et al.*, 2001).

Table 1: Composition of nine diclofenac sodium transdermal patch formulations prepared with varying polymer and excipient ratios.

Formulation	HPMC (g)	PVP (g)	PEG (g)	Drug (g)	SLS (g)
F1	1.5	1	-	0.13	0.1
F2	1.5	-	1	0.13	0.1
F3	1	1	0.5	0.13	0.1
F4	1	1.5	-	0.13	0.1
F5	-	1.5	1	0.13	0.1
F6	0.5	1.5	0.5	0.13	0.1
F7	1	-	1.5	0.13	0.1
F8	-	1	1.5	0.13	0.1
F9	1.5	0.5	0.5	0.13	0.1

Table 2: Physicochemical evaluation of patches.

Formulation	Physical Appearance	Thickness of Patch (mm)	Weight of Patch (kg)	Flatness (%)	Folding Endurance	Percent Moisture Content	pH of Patch	Drug Content (%)	Tensile Strength (kg/cm^2)	Elongation at Break (mm^2)
F1	+	0.10 ± 0.34	0.29 ± 0.13	100 ± 0.14	>200	0.004 ± 0.0032	7 ± 0.12	96 ± 0.51	0.55 ± 0.15	90 ± 0.13
F2	+	0.08 ± 0.51	0.23 ± 0.17	70 ± 0.65	>200	0.003 ± 0.0046	7 ± 0.16	96 ± 0.53	0.34 ± 0.18	22 ± 0.05
F3	+	0.09 ± 0.29	0.19 ± 0.24	100 ± 0.31	>200	0.003 ± 0.0071	7 ± 0.14	97 ± 0.59	1.89 ± 0.12	102 ± 0.08
F4	+	0.10 ± 0.75	0.28 ± 0.11	100 ± 0.29	>200	0.003 ± 0.0049	7 ± 0.11	96 ± 0.52	0.99 ± 0.19	99 ± 0.11
F5	+	0.12 ± 0.28	0.27 ± 0.19	70 ± 0.24	>200	0.004 ± 0.0083	7 ± 0.19	95 ± 0.54	0.32 ± 0.11	44 ± 0.19
F6	+	0.08 ± 0.44	0.28 ± 0.32	100 ± 0.83	>200	0.005 ± 0.0027	7 ± 0.16	96 ± 0.58	0.87 ± 0.14	101 ± 0.10
F7	+	0.09 ± 0.62	0.21 ± 0.19	100 ± 0.72	>200	0.004 ± 0.0012	7 ± 0.11	97 ± 0.52	0.97 ± 0.09	99 ± 0.16
F8	+	0.07 ± 0.49	0.27 ± 0.27	80 ± 0.69	>200	0.003 ± 0.0046	7 ± 0.12	95 ± 0.54	0.45 ± 0.17	63 ± 0.04
F9	+	0.09 ± 0.62	0.25 ± 0.15	100 ± 0.34	>200	0.004 ± 0.0093	7 ± 0.14	96 ± 0.50	1.57 ± 0.08	96 ± 0.17

+ = satisfactory result, Values expressed as mean ± SD, n = 3.

In vitro Drug Release/Drug Permeation Study

Drug release from the transdermal patches was evaluated using a Franz diffusion cell equipped with a semi-permeable cellophane membrane. The receptor compartment was filled with phosphate buffer (pH 5.8) and maintained at 37 ± 2°C using a thermostatically controlled water jacket and magnetic stirrer to ensure uniform mixing. The patch was mounted on the membrane with the drug-loaded side facing the receptor medium. At predetermined intervals, aliquots were withdrawn and immediately replaced with fresh buffer to maintain sink conditions. Samples were analyzed spectrophotometrically at 276 nm to quantify the cumulative drug release across the membrane over time (Subedi & MeenakshiKandwal).

Release Kinetics

The release kinetics were analyzed using data from the *in vitro* drug release studies processed through the DD-Solver add-in for Microsoft Excel. The release mechanism was evaluated by fitting the data to zero-order, first-order, Higuchi, and Korsmeyer–Peppas kinetic models to determine the best-fit equation and elucidate the drug-release mechanism (Mustafa *et al.*, 2024).

Skin Compatibility Study

The dermal safety of the optimized diclofenac sodium transdermal patches was evaluated in six healthy albino rats weighing 200-250 g, divided equally into control (n = 3) and test (n = 3) groups. All procedures were approved by the Institutional Animal Ethics Committee and conducted in compliance with ARRIVE guidelines with Approval No. FOPS-DP/0145; 19 November 2024). The dorsal surface of each rat's thigh of each rat was shaved 24 hr before dosing. A patch (2 × 2 cm^2) containing diclofenac sodium was applied to the shaved region and secured with hypoallergenic adhesive tape and gauze to maintain occlusion. Blank patches served as controls. Patches were removed after 24 hr, and the application sites were examined visually at 1, 24, 48, and 72 hr post-removal. Erythema and edema were scored using the Draize scale (0–4), and the Primary Irritation Index (PII) was calculated as the mean of all scores (Abdul Rasool *et al.*, 2021).

RESULTS

Standard calibration curve

The standard dilutions were observed at 276 nm using a UV spectrophotometer. Figure 1 represents the calibration curve of diclofenac sodium.

Physicochemical Analysis

The physicochemical properties of all nine formulations (F1–F9) are summarized in Table 2, including physical appearance, thickness, weight uniformity, flatness, folding endurance, moisture content, surface pH, drug content, tensile strength, and percentage elongation. All patches exhibited satisfactory physical appearance without cracks or air bubbles. The thickness ranged from 0.07 mm (F8) to 0.12 mm (F5), while the weight varied between 0.19 g and 0.29 g. Most formulations demonstrated 100% flatness, except F2 (70%), F5 (70%), and F8 (80%). Folding endurance exceeded 200, indicating good flexibility. Moisture absorption was minimal (0.003–0.005%), and all formulations exhibited a surface pH of 7, confirming skin compatibility. Drug content uniformity ranged from 95% to 97%, while tensile strength varied between 0.32 ± 0.05 kg/cm^2 (F5) and 1.89 ± 0.05 kg/cm^2 (F3), with percentage elongation from 22 ± 0.03% (F2) to 102 ± 0.03% (F3).

Fourier Transform Infrared Spectroscopy (FTIR) Analysis

FTIR analysis was performed on pure diclofenac sodium, as well as drug-loaded and unloaded patches, using standard FTIR equipment. The resulting FTIR spectra are shown in Figures 2, 3, and 4.

Thermal Analysis

The DSC (differential scanning calorimetry) thermograms are presented as a blue line in Figure 2 (II). As seen in the Figure

Table 3: Release kinetics parameters of Diclofenac sodium transdermal patches.

Formulation	Zero Order		First Order		Higuchi		Korsmeyer	
	KO	R(square)	K1	R(square)	kH	R(square)	kKP	n
F1	9.188	0.9774	0.148	0.985	23.172	0.962	17.966	0.645
F2	9.917	0.9313	0.164	0.8661	24.818	0.9265	16.649	0.727
F3	10.23	0.9556	0.17	0.8621	25.497	0.9112	15.662	0.776
F4	10.865	0.989	0.192	0.8471	27.234	0.9307	18.88	0.708
F5	11.012	0.9435	0.194	0.8417	27.506	0.9189	17.695	0.75
F6	10.806	0.9822	0.182	0.9318	26.709	0.824	13.463	0.885
F7	9.521	0.9544	0.15	0.9486	23.714	0.9019	14.221	0.789
F8	9.56	0.9615	0.151	0.9485	23.759	0.8906	13.545	0.817
F9	9.953	0.9411	0.164	0.9675	24.9	0.9318	16.558	0.731

2(II)(a), diclofenac sodium demonstrates two sharp endothermic peaks at temperatures of 80°C and 285°C, immediately followed by an exothermic event at 320°C. DSC analysis in the Figure 2(II)(b) of the unloaded patch shows an endothermic trough at 50°C, an exothermic peak at 320°C and a broad endothermic peak centred at 420°C. Lastly, in the Figure 2(II)(c) drug-loaded patch shows endotherm at 80°C, an upward curve at 360°C, representing an exothermic event and a small endothermic process at 435°C. The TGA (thermogravimetric analysis) of the patches are depicted as green lines in Figure 2(I). The thermogravimetric curve for the drug, as in Figure 2(I)(c), represents initial weight loss (20%), ranging from 0-90°C, a plateau region from 100-275°C representing thermal stability, thermal degradation extending from 275°C till 350°C (25% weight loss) and completes at 500°C. TGA studies of the unloaded patch, as in Figure 2(I)(b), show initial weight loss (15%), ranging from 0-130°C, thermal stability region extending from 130°C till 265°C, thermal degradation (265-440°C) resulting in 60% weight loss and concluding at 500°C. Lastly, the diclofenac sodium-loaded patch thermogram, as in Figure 2(II)(a) reports an initial 15% weight loss up to 150°C, a thermostable region (150-250°C) and an extensive 70% weight loss due to thermolysis, ranging from 250-460°C, reaching its endpoint at 500°C.

Scanning Electron Microscopy (SEM)

The analysis focused on surface morphology, microstructure, and matrix of the prepared formulations. The matrix images obtained from SEM analysis are shown in Figures 4 (a) and (b).

In vitro Dissolution

In vitro dissolution testing was carried out using a standard dissolution apparatus for 9 hr. Table 4 presents the transdermal drug release data of formulations F1 to F9. The minimum and maximum drug release among all the formulations were 72.49% and 94.57%, respectively. The overall drug release duration was 9 hr. The transdermal drug release data are shown in Figure 5.

Release Kinetics

In the conducted experiment zero order kinetics exhibits high R^2 values ranging from (0.9313-0.989) compared to the first-order kinetics that ranges from (0.871 – 0.985) and the higuchi model ranging from (0.84 – 0.962). F4 showed the highest R^2 value (0.989) in the Zero-order model, suggesting it is independent of concentration which shows it follows zero order kinetics. The Higuchi model showed good fitting across all patches, highlighting a diffusion-controlled mechanism. Additionally, Korsmeyer–Peppas "n" values indicated non-Fickian diffusion for all formulations, meaning drug release occurs via both diffusion and polymer matrix erosion. Formulation F6, with an n value of 0.885, demonstrated the highest deviation toward polymer-controlled (Case II) transport. The corresponding data are provided in Table 3.

Skin Compatibility Test

Only negligible erythema was observed in a few animals during the first 24 hr, which subsided without progressing to edema. Mean Draize scores for erythema and edema remained below 0.3 throughout the observation period, resulting in a Primary Irritation Index (PII) < 0.4 as described in Table 4. According to Draize classification, this indicates that the patches are

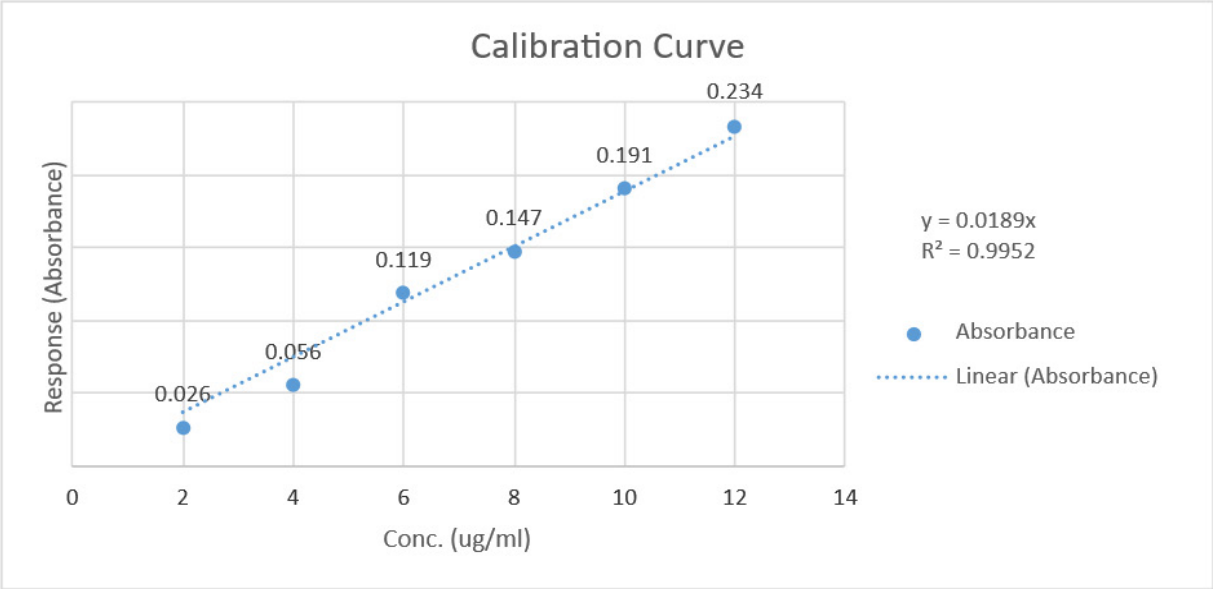

Figure 1: Calibration Curve of Diclofenac Sodium.

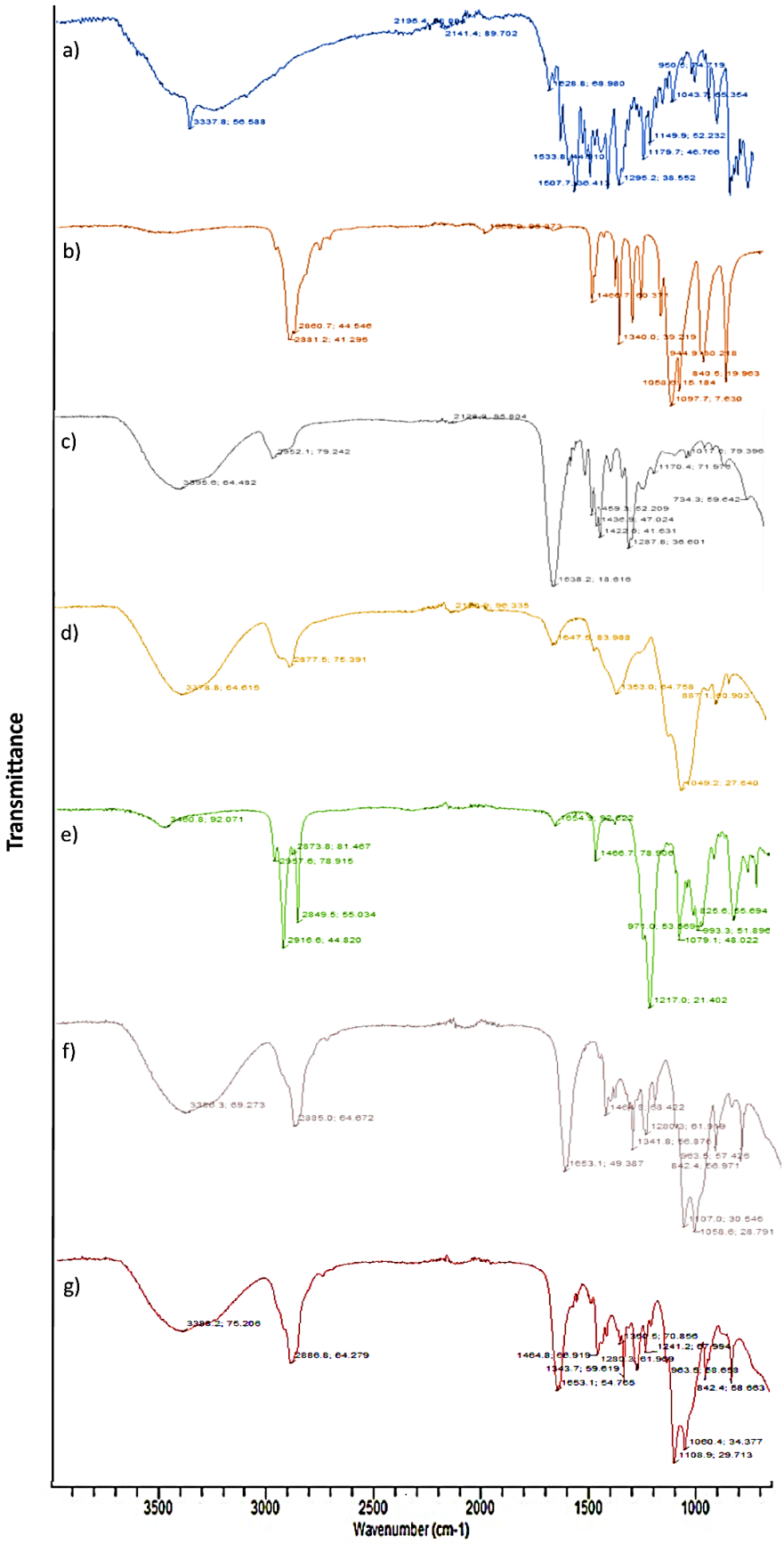

Figure 2: FTIR spectra of (a) Diclofenac sodium, (b) PEG-6000, (c) PVP-K30, (d) HPMC, (e) SLS, (f) Unloaded transdermal patch, and (g) Diclofenac sodium-loaded transdermal patch.

non-irritant. Figure 6 shows the non-irritating outcome of patches.

DISCUSSION

All formulations demonstrated satisfactory physical attributes, featuring a smooth and homogenous surface. The thickness ranged from 0.07 mm (F8) to 0.12 mm (F5), and the weight varied from 0.19 g (F3) to 0.29 g (F1). These results align with Shailesh *et al.*, (2011), who reported similar uniformity and film quality in repaglinide transdermal patches (Shailesh T *et al.*, 2011). Most formulations (seven patches) had consistent strip dimensions before and after cutting, indicating 100% flatness. This absence of constriction enables maintenance of a uniform surface while application, promoting close contact and improved drug permeation. F8 had 80% flatness, while F2 and F5 showed 70% flatness, representing manufacturing inconsistencies. The folding endurance exceeded 200, exhibiting optimum flexibility and integrity with skin folding when applied, without brittleness. Minimal moisture absorption (0.003-0.005%) confirms stability and antimicrobial preservation. The neutral surface pH of 7 ensures excellent biocompatibility. Consistent drug loading across all formulations was confirmed by the drug content analysis, which ranged from 95% to 97%. Tensile strength was found to be in the range of 0.32 ± 0.05 kg/cm^2 (F5) to 1.89 ± 0.05 kg/cm^2 (F3) and % elongation between 22 ± 0.03% (F2) and 102 ± 0.03% (F3), Findings align with Kim and Choi (2021), confirming that optimal mechanical strength, flatness, and minimal moisture uptake ensure stable, flexible, and biocompatible transdermal patches (Zhang *et al.*, 2014; Kim & Choi, 2021).

In the diclofenac sodium sample, the moderate-intensity peaks were observed at 3337.8 cm^{-1} (with 56.588 transmittances) and 1628.68 cm^{-1} (with 68.980 transmittances), respectively, interpreting the functional groups of COOH and C=C, respectively, as shown in Figure 2 (a). A study conducted in 2021 reported similar results for diclofenac sodium, confirming the presence of the COOH and C=C functional groups within the official range (Suhail *et al.*, 2021). The strong intensity peaks of PEG 6000 were observed at 2881.2 cm^{-1} (with a transmittance of 41.295) for the C-H group and at 1097.7 cm^{-1} (with a transmittance of 7.630) for the C-O-C group, as shown in Figure 2 (b). These findings are consistent with those conducted in 2020, which demonstrated the presence of C-H and C-O-C groups (Bhatia & Devi, 2020). PVP K-30, a moderate intensity peak appeared at 3395.6 cm^{-1} (with 64.482 transmittance) for the N-H group at 1638.2 cm$^{-1,}$ the peak was strong (with 18.616 transmittance) and was attributed to the C=O group, as shown in Figure 2 (c). In the research conducted in 2020, similar peaks for C-O-C and C=O groups were reported, indicating that our findings fall within the limit (Febriyenti *et al.*, 2020). The moderate intensity peak in the HPMC sample was observed at 3378.8 cm^{-1} (with 64.615 transmittance) for the -OH group and the strong intensity peak at 1049.2 cm^{-1} (with 27.640 transmittance) for the C-O-C group, as shown in Figure 2 (d). A study conducted in 2020 provides similar results, which proves the presence of the O-H group and the C-O-C functional group, both showed their peak intensities and transmittances at the points aligned with our research, and fall within the official limits (Alshehri *et al.*, 2020). In the SLS, the sample strong stretching band for the C-H group is present at 2916.6 cm-1 with a transmittance of 44.820, and for the S=O group, a strong stretching band is present at 1217.0 cm^{-1} with a transmittance of 21.402, as shown in Figure 2 (e). In the SLS, the peaks and transmittances of the groups C-H and S=O are similar to the study considered as a reference here, conducted in 2021. Both studies' results are within the official standards (Kharroubi *et al.*, 2021). In the unloaded transdermal patch, the stretching vibration of PEG 6000 is shown at 2885.0 cm^{-1} (C-H group), the peak of PVP K-30 is observed at 3386.3 cm^{-1} (N-H group), and the stretching band of HPMC is at 1058.6 cm^{-1} (ether group) in the patch, as shown in Figure 2 (f). The peaks of polymer in the loaded patch (containing diclofenac sodium) are slightly shifted due to the presence of the drug. The peaks of the drug, PEG 6000, PVP K-30, and HPMC in the loaded patch are present at 1653.1 cm^{-1}, 2886.8 cm^{-1}, 3388.2 cm^{-1}, and 1060.4 cm^{-1}, respectively, as shown in Figure 2 (g).

The DSC thermogram of diclofenac sodium in Figure 3(II) (a) exhibited two endothermic peaks at 80°C and 285°C, corresponding to polymorphic transition and melting, followed by an exothermic peak due to oxidative degradation, consistent with (Tita *et al.*, 2009). In contrast, the unloaded patch in Figure 3(II)(b) showed a minor endotherm between 50–100°C from moisture loss of hygroscopic polymers (HPMC, PVP K-30, PEG-6000), and a broad exotherm at 320–420°C reflecting polymer decomposition, aligning with (Bolourchian *et al.*, 2019; Krause *et al.*, 2023; Mummidi & Jayanthi, 2013). The drug-loaded patch in Figure 3(II)(c) exhibited a similar initial endotherm (50–100°C) but lacked the sharp melting peak of diclofenac sodium, indicating amorphous dispersion and drug–polymer interaction.

Table 4: Draize scores for erythema and edema following application of diclofenac sodium transdermal patches in rats (*n* = 3).

Time after patch removal (h)	Erythema (Mean ± SD)	Edema (Mean ± SD)	Primary Irritation Index (PII)
1 hr	0.2 ± 0.1	0.1 ± 0.0	0.15
24 hr	0.3 ± 0.2	0.1 ± 0.1	0.20
48 hr	0.1 ± 0.1	0.0 ± 0.0	0.05
72 hr	0.0 ± 0.0	0.0 ± 0.0	0.00

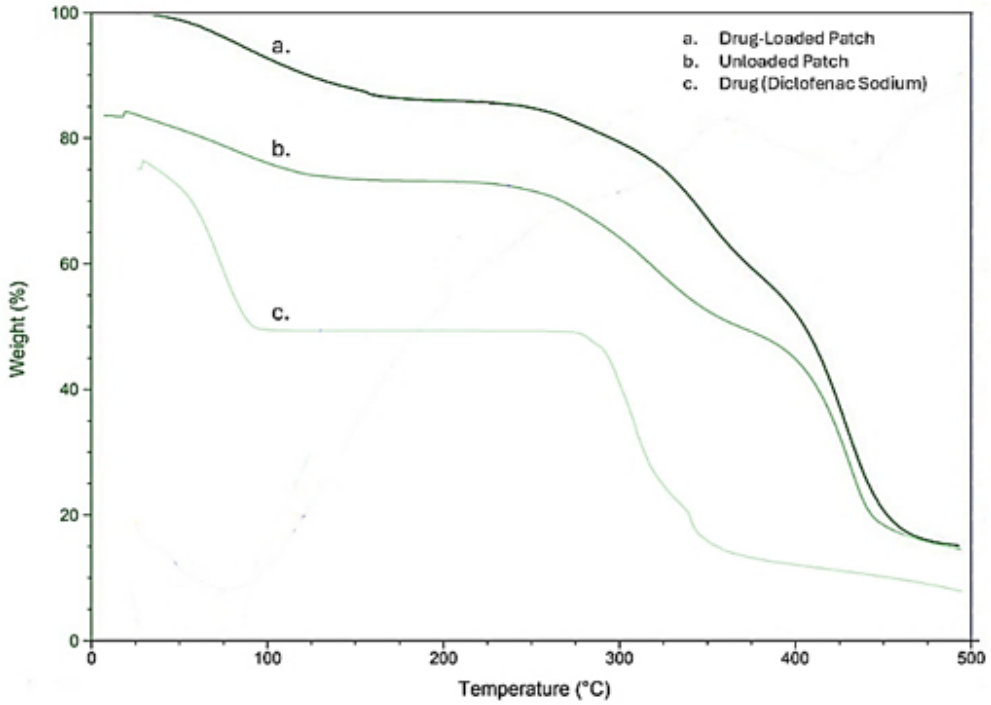

(I)

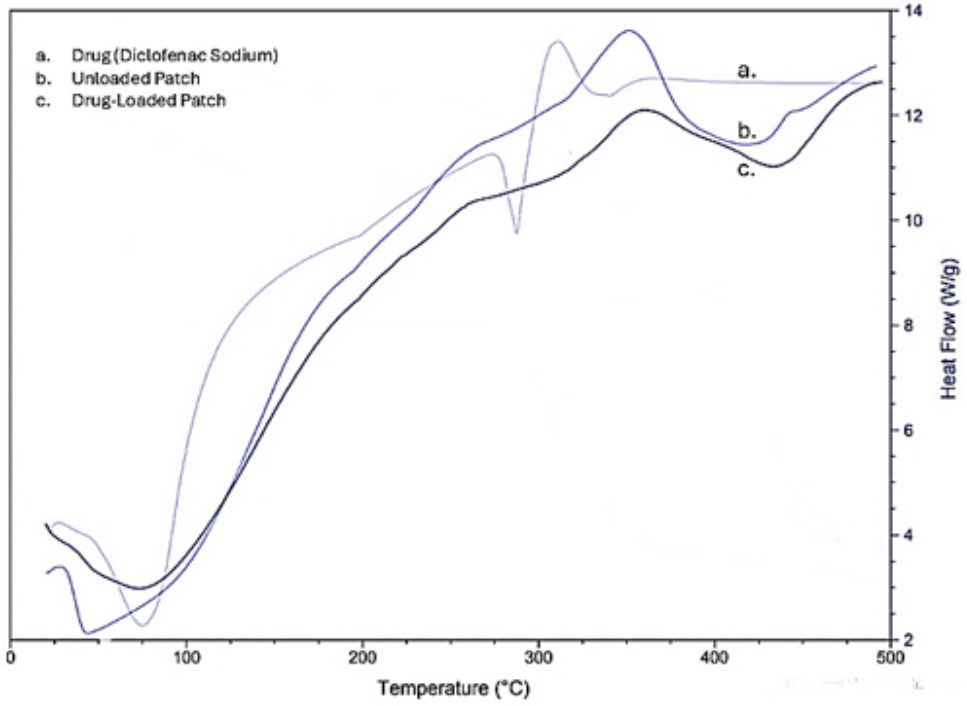

(II)

Figure 3: (I) Thermogravimetric Analysis (TGA) curves of (a) drug-loaded patch, (b) unloaded patch, and (c) pure drug. (II) Differential Scanning Calorimetry (DSC) curves of (a) pure drug, (b) unloaded patch, and (c) drug-loaded patch.

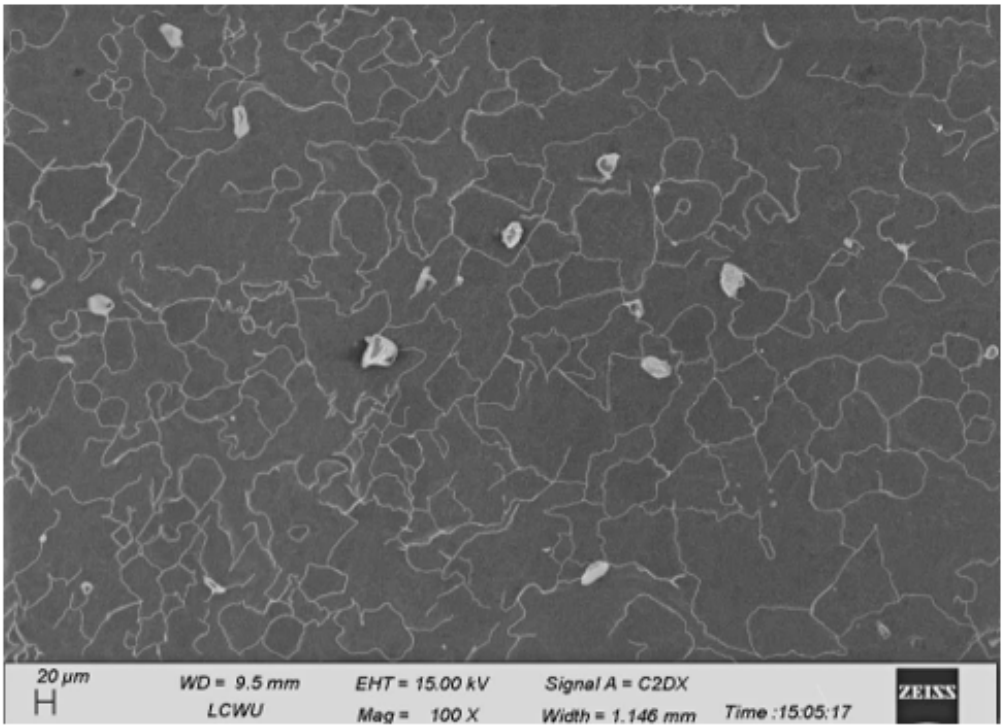

(a)

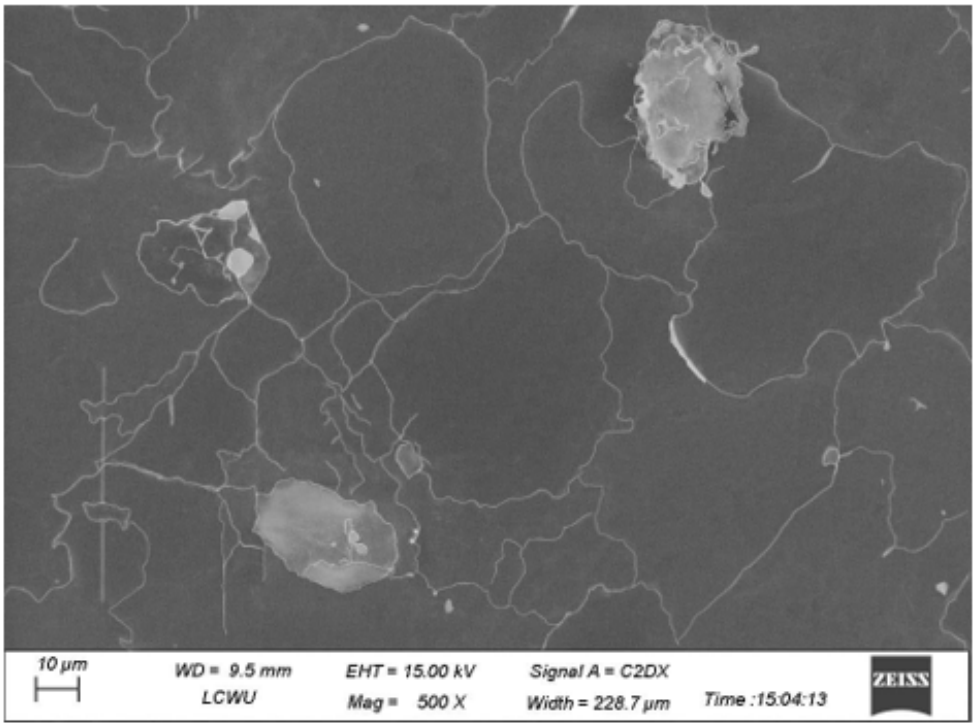

(b)

Figure 4: SEM images of transdermal patches. (a) Surface morphology of the unloaded patch at 100× magnification (scale bar = 20 µm; working distance = 9.5 mm; EHT = 15.00 kV). (b) Surface morphology of the drug-loaded patch at 500× magnification (scale bar = 10 µm; working distance = 9.5 mm; EHT = 15.00 kV).

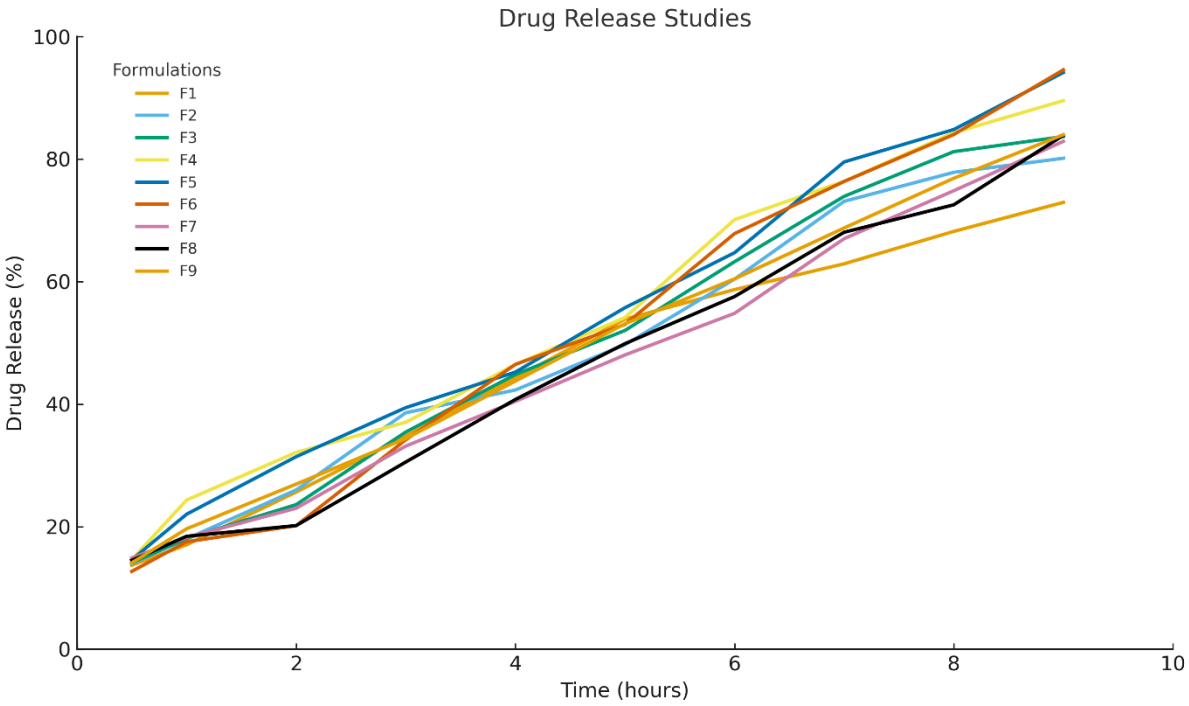

Figure 5: *In vitro* drug release profile of the Diclofenac sodium transdermal patch.

A broad exotherm near 360°C confirmed simultaneous degradation of the drug and polymer matrix.

TGA further supported these observations. Pure diclofenac sodium in Figure 3(I)(c) showed ~20% weight loss up to 90°C (moisture loss) and major degradation between 275–350°C, in agreement with (Tudja *et al.*, 2001). The unloaded patch in Figure 3(I)(b) remained stable up to 265°C, with ~60 % weight loss from 265–440°C due to polymer breakdown as observed by (Redondo *et al.*, 2022). The drug-loaded patch in Figure 3(I)(a) exhibited slightly lower onset stability but higher total weight loss (~70%) from 250–460°C, confirming combined decomposition and strong matrix integration. Collectively, the DSC and TGA profiles demonstrate multi-stage degradation typical of HPMC/PVP/PEG systems, verifying thermal compatibility, uniform dispersion, and formation of a stable amorphous drug–polymer matrix suitable for transdermal delivery.

SEM analysis confirmed uniform drug distribution within the polymeric matrix. DS-loaded patches (10 µm, 50×) showed a smooth, homogeneous surface with slight irregularities, indicating proper dispersion and facilitating easier drug release as the similar SEM scans were observed by (Arora & Mukherjee, 2002).

Within the first 3 hr, F1–F3 released 34.80%, 38.60%, and 35.45% of the drug, while F4–F6 showed slightly higher values (37.04%, 39.43%, 34.18%), and F7–F9 released 33.15%, 30.05%, and 34.38%. At 3 hr, F5 exhibited the highest cumulative release. Between 4–6 hr, F1–F3 reached 58.70–63.25%, F4–F6 64.72–70.12%, and F7–F9 54.82–60.45%, with F4 showing the fastest diffusion. At 9 hr, cumulative release rose to 72.94–83.68% (F1–F3), 89.54–94.57% (F4–F6), and 82.90–83.98% (F7–F9), with F5 achieving the maximum. The overall release order was F6 > F5 > F4 > F9 > F7 > F8 > F3 > F2 > F1. Formulations F5 and F6 showed superior, sustained release due to the synergistic HPMC–PVP polymer blend enhancing matrix integrity, hydration, and controlled diffusion (Jaber, 2023).

The comparison of R^2 values (Table 5) revealed that the zero-order kinetic model exhibited the strongest correlation with experimental data (R^2 = 0.9313–0.989), outperforming the first-order model (0.871–0.985). Among all, formulation F4 showed the highest R^2 (0.989) under the zero-order model, indicating a constant, concentration-independent release rate. This pattern aligns with the ideal behavior of transdermal systems, providing a steady and predictable delivery profile. Overall, these results confirm that diclofenac sodium release followed zero-order kinetics, enabling prolonged and controlled drug release, with F4 displaying the most favorable performance (Barros *et al.*, 2015). A high R^2 values for Higuchi indicating that diffusion plays a key role in drug release from the polymeric matrix. Korsmeyer-Peppas model further supported this with n values between 0.645 and 0.885, confirming non-Fickian (anomalous) diffusion in all cases (Mustafa *et al.*, 2024).

The diclofenac sodium transdermal patches demonstrated excellent dermal safety, as reflected by Draize scores consistently below 0.3 and a Primary Irritation Index < 0.4. These findings place the formulation in the non-irritant category, confirming the absence of clinically significant erythema or edema. The slightly transient erythema noted within the first 24 h may be attributed

Figure 6: Assessment of dermal tolerance of transdermal patches following topical application on male albino rats.

to occlusion or the adhesive material rather than the active formulation. These results align with Abdullah *et al*., (2023), who reported that diclofenac sodium transdermal patches caused no erythema or edema in rats, confirming their dermal safety and non-irritant nature (Abdullah *et al*., 2023). The results indicate that the developed diclofenac sodium patches are dermally safe and biocompatible.

CONCLUSION

This study establishes an optimized transdermal delivery platform for diclofenac sodium using a synergistic polymeric matrix of HPMC, PVP K-30, PEG-6000, and SLS. The films demonstrated excellent physicochemical uniformity, mechanical strength, and stability, reflecting formulation reliability. FTIR and DSC analyses confirmed drug–polymer compatibility, while SEM imaging revealed a uniform microstructure favorable for controlled diffusion. Sustained drug release was achieved for up to 9 hr, with formulation F6 showing the highest cumulative release (94.57%). Kinetic modeling indicated zero-order, non-Fickian behavior, suggesting a dual mechanism of diffusion and polymer relaxation. Dermal safety testing showed no erythema or edema, with Draize and PII scores confirming the system as non-irritant and biocompatible. Collectively, these findings highlight a clinically promising alternative to oral or injectable diclofenac therapy, capable of providing prolonged analgesic action, improved patient compliance, and reduced gastrointestinal risks. The developed transdermal system thus represents a significant step toward safer, more effective management of chronic musculoskeletal pain, warranting further *in vivo* and clinical validation for translational applications.

ACKNOWLEDGEMENT

We sincerely appreciate the Deanship of the Faculty of Pharmaceutical Sciences at Lahore University of Biological and Applied Sciences (UBAS) for their invaluable support and provision of essential resources that facilitated this research. Their dedication to academic excellence and research advancement has been instrumental in the successful completion of this study.

ABBREVIATIONS

XRD: X-ray Diffraction; **API:** Active Pharmaceutical Ingredient; **DSC:** Differential Scanning Calorimetry; **TGA:** Thermogravimetric Analysis; **UV-vis:** Ultraviolet-visible Spectroscopy; **SEM:** Scanning Electron Microscope; **SLS:** Sodium Lauryl Sulfate; **DS:** Diclofenac Sodium.

CONFLICT OF INTEREST

The authors declare that there is no conflict of interest.

REFERENCES

Abdul M. R. (2025). Validation and Development of UV spectroscopy method for the Estimation of Diclofenac sodium in Bulk and dos protected mode interface. *Misan Journal of Academic Studies* 24(53) https://doi.org/10.54633/2333-024-053-013

Abdul Rasool B. K., Mohammed A. A., Salem Y. Y. (2021). The optimization of a dimenhydrinate transdermal patch formulation based on the quantitative analysis of *in vitro* release data by DDSolver through skin penetration studies. *Scientia Pharmaceutica* 89(3): 33 https://doi.org/10.3390/scipharm89030033

Abdullah H. M., Farooq M., Adnan S., Masood Z., Saeed M. A., Aslam N., Ishaq W. (2023). Development and evaluation of reservoir transdermal polymeric patches for controlled delivery of diclofenac sodium. *Polymer Bulletin* 80(6): 6793–6818 https://doi.org/10.1007/s00289-022-04390-0

Adamiak-Giera U., Gackowski M., Szostak J., Osmałek T., Malinowski D., Nowak A., Machoy-Mokrzyńska A., Miernik M., Halczak M., Romanowski M. (2025). Evaluation of the *in vitro* Permeation Parameters of Topical Diclofenac Sodium from Transdermal

Pentravan® Products and Hydrogel Celugel Through Human Skin. *Pharmaceuticals* 18(6): 810 https://doi.org/10.3390/ph18060810

Akhtar N., Singh V., Yusuf M., Khan R. A. (2020). Non-invasive drug delivery technology: Development and current status of transdermal drug delivery devices, techniques and biomedical applications. *Biomedical Engineering/Biomedizinische Technik* 65(3): 243–272 https://doi.org/10.1515/bmt-2019-0019

Alkilani, A. Z., McCrudden, M. T. C., & Donnelly, R. F. (2015). Transdermal drug delivery: Innovative pharmaceutical developments based on disruption of the barrier properties of the stratum corneum. *Pharmaceutics*, 7(4), 438–470.

https://doi.org/10.3390/pharmaceutics7040438

Alkilani A. Z., Nasereddin J., Hamed R., Nimrawi S., Hussein G., Abo-Zour H., Donnelly R. F. (2022). Beneath the skin: a review of current trends and future prospects of transdermal drug delivery systems. *Pharmaceutics* 14(6): 1152 https://doi.org/10.3390/pharmaceutics14061152

Alshehri S., Imam S. S., Hussain A., Altamimi M. A. (2020). Formulation of piperine ternary inclusion complex using β-CD and HPMC: physicochemical characterization, molecular docking, and antimicrobial testing. *Processes* 8(11): 1450 https://doi.org/10.3390/pr8111450.

Arora P., Mukherjee B. (2002). Design, development, physicochemical, and *in vitro* and *in vivo* evaluation of transdermal patches containing diclofenac diethylammonium salt. *Journal of Pharmaceutical Sciences* 91(9): 2076–2089 https://doi.org/10.1002/jps.10200

Barros, N. R. D., Chagas, P. A. M., Borges, F. A., Gemeinder, J. L. P., Miranda, M. C. R., Garms, B. C., & Herculano, R. D. (2015). Diclofenac potassium transdermal patches using natural rubber latex biomembranes as carrier.*Journal of Materials*,*2015*(1), 807948 https://doi.org/10.1155/2015/807948

Bhatia M., Devi S. (2020). Development, characterisation and evaluation of PVP K-30/PEG solid dispersion containing ketoprofen. *ACTA Pharmaceutica Sciencia* 58(1) https://doi.org/10.23893/1307-2080.APS.05806

Bolourchian N., Talamkhani Z., Nokhodchi A. (2019). Preparation and physicochemical characterization of binary and ternary ground mixtures of carvedilol with PVP and SLS aimed to improve the drug dissolution. *Pharmaceutical Development and Technology* 24(9): 1115–1124 https://doi.org/10.1080/10837450.2019.1641516

Brogden R., Heel R., Pakes G., Speight T. M., Avery G. (1980). Diclofenac sodium: a review of its pharmacological properties and therapeutic use in rheumatic diseases and pain of varying origin. *Drugs* 20(1): 24–48 https://doi.org/10.2165/00003495-198020010-00002

Cui A., Li H., Wang D., Zhong J., Chen Y., Lu H. (2020) Global, regional prevalence, incidence and risk factors of knee osteoarthritis in population-based studies. *EClinical Medicine* 29–30: 100587 https://doi.org/10.1016/j.eclinm.2020.100587

Febriyenti P. I., Zaini E., Ismed F., Lucida H. (2020). Preparation and characterization of quercetin-polyvinylpyrrolidone K-30 spray dried solid dispersion. *Journal of Pharmacy and Pharmacognosy Research* 8: 127–134 https://doi.org/10.56499/jppres19.729_8.2.127

Fong Yen W., Basri M., Ahmad M., Ismail M. (2015). Formulation and evaluation of galantamine gel as drug reservoir in transdermal patch delivery system. *The Scientific World Journal* 2015(1): 495271 https://doi.org/10.1155/2015/495271

Jaber S. A. (2023). Transdermal patches based on chitosan/hydroxypropyl methylcellulose and polyvinylpyrrolidone/hydroxypropyl methylcellulose polymer blends for gentamycin administration. *Journal of Advanced Pharmaceutical Technology & Research* 14(3): 202–207 https://doi.org/10.4103/japtr.japtr_130_23

Kharroubi M., Bellali F., Karrat A., Bouchdoug M., Jaouad A. (2021). Preparation of *Teucrium polium* extract-loaded chitosan-sodium lauryl sulfate beads and chitosan-alginate films for wound dressing application. *AIMS Public Health* 8(4): 754 https://doi.org/ 10.3934/publichealth.2021059

Kim E. J., Choi D. H. (2021). Quality by design approach to the development of transdermal patch systems and regulatory perspective. *Journal of Pharmaceutical Investigation* 51(6): 669–690 https://doi.org/ 10.1007/s40005-021-00536-w

Krause B., Imhoff S., Voit B., Pötschke P. (2023). Influence of polyvinylpyrrolidone on thermoelectric properties of melt-mixed polymer/carbon nanotube composites. *Micromachines* 14(1): 181 https://doi.org/10.3390/mi14010181

Kumar S. S., Behury B., Sachinkumar P. (2013). Formulation and evaluation of transdermal patch of Stavudine. *Dhaka University Journal of Pharmaceutical Sciences* 12(1): 63–69 https://doi.org/ 10.3329/dujps.v12i1.16302

Mamatha J., Gadili S., Pallavi K. (2020). Formulation and evaluation of zidovudine transdermal patch using permeation enhancers. *Journal of Young Pharmacists* 12(2s): S45 https://doi.org/ 10.5530/jyp.2020.12s.45

Mummidi V., Jayanthi V. (2013). Effect of hydrophilic polymers on isradipine complexation with hydroxypropyl β-cyclodextrin. *Drug Development and Industrial Pharmacy* 39(7): 970–977 https://doi.org/ 10.3109/03639045.2012.686508

Mustafa M. A., Farooq H., Asif E., Saleem A., Amin M., Shafiq H., Shabbir A., Anwar H., Mahmood M., Ahsan M. S. (2024). Design, Fabrication and Characterization of Transdermal Patches Using Different Natural Polymers Containing Caffeine and Ibuprofen for Long-Term Management of Migraine. *International Journal of Pharmaceutical Investigation* 14(4) https://doi.org/10.5530/ijpi.14.4.130

Nayak B. S., Ellaiah P., Pattanayak D., Das S. (2011). Formulation design preparation and *in vitro* characterization of nebivolol transdermal patches. *Asian Journal of Pharmaceutics* 5(3) https://doi.org/10.22377/ajp.v5i3.104

Prajapati S. T., Patel C. G., Patel C. N. (2011). Formulation and evaluation of transdermal patch of repaglinide. *International Scholarly Research Notices* 2011(1): 651909 https://doi.org/ 10.5402/2011/651909

Ramadon D., McCrudden M. T., Courtenay A. J., Donnelly R. F. (2022). Enhancement strategies for transdermal drug delivery systems: Current trends and applications. *Drug Delivery and Translational Research* 12(4): 758–791 https://doi.org/ 10.1007/s13346-021-00909-6

Redondo D. C. V., Leite E. C., da Silva A. R. J., da Silva B. B., Guimarães M. (2022). Microstructured drug-delivery systems as solid dispersions using PEG 6000 and polysorbate 80 containing hydrochlorothiazide: development, synthesis, and physicochemical and morphological characterization. *Brazilian Journal of Natural Sciences* 4(3): E1662022–1662012 https://doi.org/ 10.31415/bjns.v4i3.166

Shafique N., Siddiqui T., Zaman M., Iqbal Z., Rasool S., Ishaque A., Siddique W., Alvi M. N. (2021). Transdermal patch co-loaded with Pregabalin and Ketoprofen for improved bioavailability; *in vitro* studies. *Polymers and Polymer Composites* 29(9_suppl): S376–S388 https://doi.org/ 10.1177/09673911211004516

Sin A., Hollabaugh W., Porras L. (2025). Narrative review and call to action on reporting and representation in orthobiologics research for knee osteoarthritis. *PM&R* 17(1): 88–95 https://doi.org/ 10.1002/pmrj.13214

Singh A., Bali A. (2016). Formulation and characterization of transdermal patches for controlled delivery of duloxetine hydrochloride. *Journal of Analytical Science and Technology* 7(1): 25 https://doi.org/ 10.1186/s40543-016-0105-6

Singh V., Devi M., Verma K. K. (2024). A Review article on Diclofenac Sodium Topical gel on Osteoarthritis. *Research Journal of Topical and Cosmetic Sciences* 15(1): 53–59 https://doi.org/ 10.52711/2321-5844.2024.00010

Suhail M., Wu P.-C., Minhas M. U. (2021). Development and characterization of pH-sensitive chondroitin sulfate-co-poly (acrylic acid) hydrogels for controlled release of diclofenac sodium. *Journal of Saudi Chemical Society* 25(4): 101212 https://doi.org/ 10.1016/j.jscs.2021.101212

Tita B., Fulias A., Marian E., Tita D. (2009). Thermal stability and decomposition kinetics under non-isothermal conditions of sodium diclofenac. *Pharmaceuticals* 12: 14 https://doi.org/ 10.37358/Rev.Chim.1949

Törnblom M., Bremander A., Aili K., Andersson M. L., Nilsdotter A., Haglund E. (2024). Development of radiographic knee osteoarthritis and the associations to radiographic changes and baseline variables in individuals with knee pain: a 2-year longitudinal study. *BMJ Open* 14(3): e081999 https://doi.org/10.1136/bmjopen-2023-081999

Tudja P., Khan M. Z. I., MEŠTROVIC E., Horvat M., Golja P. (2001). Thermal behaviour of diclofenac sodium: decomposition and melting characteristics. *Chemical and Pharmaceutical Bulletin* 49(10): 1245–1250 https://doi.org/ https://doi.org/10.1248/cpb.49.1245

Wolff D. G., Christophersen C., Brown S. M., Mulcahey M. K. (2021). Topical nonsteroidal anti-inflammatory drugs in the treatment of knee osteoarthritis: a systematic review and meta-analysis. *The Physician and Sportsmedicine* 49(4): 381–391 https://doi.org/10.1080/00913847.2021.1886573

Zhu S., Qu W., He C. (2024). Evaluation and management of knee osteoarthritis. *Journal of Evidence-Based Medicine* 17(3): 675–687 https://doi.org/10.1111/jebm.12627

Zhang, Y., Cun, D., Kong, X., & Fang, L. (2014). Design and evaluation of a novel transdermal patch containing diclofenac and teriflunomide for rheumatoid arthritis therapy.*Asian* Journal of pharmaceutical *sciences*,*9*(5), 251-259 https://doi.org/10.1016/j.ajps.2014.07.007

Cite this article: Mustafa MA, Khan AM, Atif A, Wajid F, Ali N, Ashfaq K, *et al*. Fabrication and *in vitro-ex vivo* Evaluation of Diclofenac Sodium Transdermal Patches for Enhanced Skin Compatibility. Int. J. Pharm. Investigation. 2026;16(3):1005-17.